Proceedings of the ASME 2010 3rd Joint US-European Fluids Engineering Summer Meeting and 8th International Conference on Nanochannels, Microchannels, and Minichannels
FEDSM-ICNMM2010
August 1-5, 2010, Montreal, Canada

FEDSM-ICNMM2010-30992

EFFECT OF LONGITUDINAL VORTEX ON BOUNDARY LAYER STATE AND SEPARATION ON NACA SYMMETRIC FOIL

Sebastien Prothin
IRENav – French Naval Academy
Lanvéoc, France
Email: sebastien.prothin@ecole-navale.fr

Henda Djeridi
Laboratoire de Physique des Océans (UMR 6523)
UBO / UFR Sciences
Brest, France
Email: henda.djeridi@univ-brest.fr

Jean-Yves Billard
IRENav – French Naval Academy
Lanvéoc, France
Email: jean-yves.billard@ecole-navale.fr

ABSTRACT

Vortex generators have been widely used in aerodynamics to control the separation of boundary layers. In such application (Angele and Muhammad, 2005) vortex generators are embedded in the boundary layer and the vortex height, with regards to the wall, is of the boundary layer thickness. The objective of this configuration is obviously far from being the effects of a single longitudinal vortex (generated upstream by an elliptical plan form profile) on the turbulent boundary layer shape over a Naca0015 symmetric foil at different incidences at high Reynolds number 5 10^5. The vortex is situated outside the boundary layer (ten times the BL thickness over the wall) taking into account the small value of the thickness in our hydrodynamic application. Obviously, this situation is optimum as the vortex delays separation and increases the maximum lift but introduces drag penalty at small incidence. This is nevertheless frequently encountered in hydrodynamic applications (hub vortex upstream of a rudder) and of interest. To point out the mechanism of the boundary layer manipulation, both global efforts using gauge balance and velocity measurements using LDV and PIV have been performed and compared with and without vortex. The base flow is an APG boundary layer characterized by a predominant wake area. Effect of the vortex is analyzed via the shape factor both in inflow and outflow regions. The longitudinal vortex suppress the hysteretic loop classically described in this Reynolds number range (Djeridi et al., 2009) but an increase of the drag is observed in the range of incidence just before stall. Velocity measurements indicated that, for incidences near the stall appearance, the shape factor is decreased both in the inflow and in the outflow regions. Even for large incidences, in the inflow region the value of the shape factor is equivalent to the one found in the turbulent BL over a flat plate. In this region the vortex modifies the equilibrium state of the BL as attested by the Clauser parameter. Even for large distances between the vortex and the wall, the ability of the vortex to suppress the detachment of the BL is observed on the evolution of the backflow coefficient. This effect is greater pronounced in inflow area near the trailing edge region where the flow is locally reattached due to the high momentum fluid displacement.

NOMENCLATURE

(x, y, z)	cartesian coordinate [mm]
(r, θ, z)	cylindrical coordinate [mm]
c, c_{ell}	chord of 2D and 3D foil [mm]
t	maximum thickness of the foil [%]
H	height of the test section [mm]
U_e	external velocity on the normal line [m/s]
U_{inf}	infinite velocity [m/s]
δ	boundary layer thicknesses [mm]
δ_1	displacement thicknesses [mm]
δ_2	momentum thicknesses [mm]
H_{12}	classical shape factor [-]
h	shape factor for the separation [-]
χ	backflow coefficient [%]
a	effective size of the vortex core [mm]
Γ	vortex strength (circulation) [m²/s]
l	pitch of the helical vortex lines [mm]
U_0	advection velocity of the vortex [m/s]
d	position of the vortex to 2D foil [mm]
Cp_{min}	minimum of Pressure coefficient [-]

INTRODUCTION

Interaction between vortex and boundary layer can be used in control applications. In spite of this industrial interest very few studies deal with the physical mechanism which takes place in this interaction and most of the studies focus on aerodynamic applications where vortex generators are in the boundary layer. In hydrodynamic applications the vortex is generated out of the boundary layer (BL), for instance, hub vortex issued from a propeller in interaction with the downstream rudder.

Many studies have been experimentally conducted to test the effectiveness of different configuration of interactions between single vortex or vortices issue from vortex generators (VGs) and BL. Shabaka et al. [1] investigated the mean and turbulent flow of the low speed BL in zero pressure gradient (ZPG) disturbed by a longitudinal isolated vortex imbedded in it. They shown that the circulation around the vortex was almost maintained, the region of flow affected by the vortex continued to grow downstream and remained proportional to the BL thickness (δ). Mehta and Bradshaw [2] in the same configuration but with a pair of counter-rotating vortices have shown that BL was lift-up by the vortices and has shown that BL was lifted and carried away by the vortices.

Recently, Logdberg [3], Angele and Muhammad-Klingmann [4], Angele and Grewe [5], Velte et al. [6] and Velte [7] investigated the effect of VGs on separating BL for control applications. For all these studies, VGs have been imbedded in the BL with height ratio (d/δ) about unity.

The present study investigates experimentally the effects of a single longitudinal vortex generated by an elliptical plane form NACA0020 and upstream the BL with adverse pressure gradient (APG) which developed on a 2D NACA0015 foil. In the actual case, the vortex is located outside the BL and corresponding to the hydrodynamic configuration (hub vortex/ rudder) and leads each time to an efficient separation control.

This study focuses on the mean velocity distribution of turbulent boundary layers before and after static stall. Several incidences (5, 10, 12.5, 15, 20 and 25°) have been investigated and results at 15° will be presented below since this incidence value corresponds to the hysteretic behaviour associated with lift decrease (Sarraf et al. [8]).

EXPERIMENTAL SETUP

Hydrodynamic Tunnel

The experiments have been conducted in the hydrodynamic tunnel of the French Naval Academy. This facility is fitted with a 1m long and 0.192 x 0.192 m^2 square cross test section, in which a maximum velocity of 15ms^{-1} can be achieved. The turbulence intensity upstream at the entrance of the test section is 2%.

The flow characteristics correspond to the upstream Reynolds number based on NACA0015 chord length of 5.10^5. The vortex is generated by a NACA0020 foil with elliptical plan form located 2 chords upstream of the 2D foil. The characteristics of the vortex are described by Pichon [9]. The experimental configuration is shown on Figure 1. On the plan form of the 2D foil the vortex determines 2 zones namely an outflow area where the vortex induces a velocity field directed from the wall to undisturbed flow and an inflow area where the vortex induces a velocity field directed toward the foil.

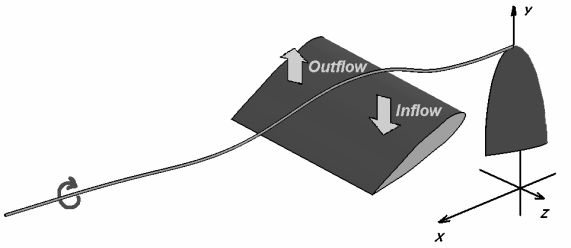

Figure 1: Experimental setup.

Laser Doppler Anemometry

To characterize the structure of the boundary layer and the near wake that develop on the 2D-hydrofoils, detailed velocity measurements was performed using a refined spatial grid by LDV (Figure 2).

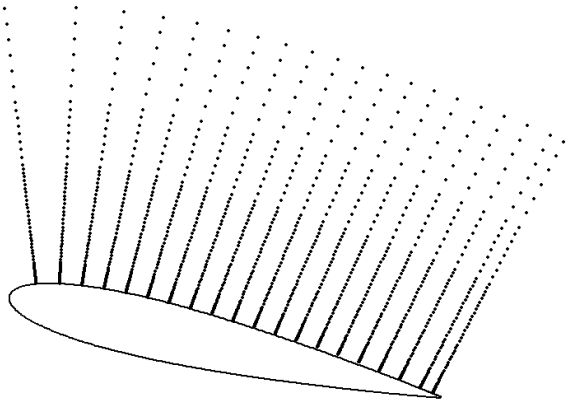

Figure 2: Refined spatial grid.

On each normal line measurements were performed from the unperturbed flow down to the wall. The spatial dimension of the probe volume (LDV) in vertical and longitudinal directions is 0.05 mm allows measurements from the outer region $y+ \sim 1000$, to the wall $y+ = 3 \sim 5$. This value corresponds to a position of the last validate point on each the normal which is positioned at 30 µm from the wall. Velocity measurements are performed from the leading to the trailing edge ($0<x/c<1$). The time histories were registered with 10 000 to 5 000 samples acquired in the range of 20 to 60 seconds corresponding to the mean data rates of 2 000 to 130 Hz. Mean and rms values of the velocity are obtained with an uncertainty of 1% and 1.5 % respectively.

Particule Image Velocimetry 2D3C

The PIV 2D3C measurements have been carried out for the NACA0015 profile at incidence 15°, 20° and 25°. A double pulse ND:YAG laser DualPower TR Lasers has been used. This delivers an energy of 2x30 mJ that illuminates silver glass particles used as flow seeding with a 1 mm thick light sheet.

The particle size is about 10 µm. Two SpeedSense 9072 cameras have been used with a resolution of 1280x800 pixels, recording double full-frame particle image. The cameras are equipped with a 60 mm objective lens at a diaphragm aperture of 1.2. The system, both camera and laser were operated at a frequency of 1000Hz. The setup is shown in Figure 3.

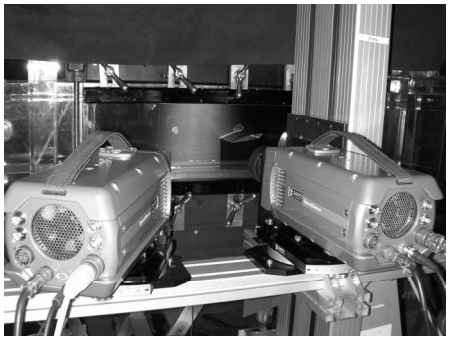

Figure 3: PIV 2D3C setup.

The size of the measurement area was -0.115 < x/c < 1.185 and -0.395 < y/c < 0.413. The flow was analyzed by cross-correlating 50% overlapping windows of 32x32 pixels.

This yield of 77x49 vectors and 1000 pairs of images was analyzed to generate converged flow fields statistics. The convergence is reached beyond an order of 500 images. Therefore, the results corresponding to 1000 images per each PIV plane provide fully converged turbulence statistics.

Gauge balance measurements

The lift and drag measurements were performed using a resistive gauge hydrodynamic balance calibrated by ourselves, with the maximum range within 0-1800 N for the lift force and 0-170 N for the drag force. The mean and root mean square (rms) values are calculated from 30 seconds test measurement carried out at 2048Hz. The determination of the hydrodynamic parameters was performed for incidence angles in the range [-20°, 30°].

FLOW CHARACTERISATION

Boundary layer with APG

For each point of measurement, 10 000 samples have been validated during a maximum of 60 s (corresponding to the near wall locations). With this number of samples, corrected convergence of mean and rms values of velocity components has been achieved. According to the previous refined grid, a survey of the distribution of mean tangential and normal velocity components is presented.

Firstly, our primary objective was to characterize the boundary shape parameters on a Naca0015 hydrofoil. Velocity profiles were numerically integrated to compute the displacement and momentum thicknesses δ_1 and δ_2, from which shape factor H_{12} is deduced. The following formulas are applied:

$$\delta_1 = \int_0^\infty \left(1 - \frac{u}{U_e}\right) dy$$

$$\delta_2 = \int_0^\infty \left(1 - \frac{u}{U_e}\right) \frac{u}{U_e} dy$$

$$H_{12} = \frac{\delta_1}{\delta_2}$$

In our confined case this velocity is the maximum velocity measured at the location.

This factor is classically used to identify the transition from laminar to turbulent. However, as H_{12} value is very high at separation, h parameter defined by Kline et al. [10] is preferred. This parameter is defined by:

$$h = \frac{H_{12} - 1}{H_{12}}$$

These authors use this parameter to characterize incipient and fully develop separations. The turbulent boundary layers which develop in ZPG conditions are characterized by a constant H_{12} value of 1.4, in those conditions h = 0.29. Kline determined two values of h that characterize incipient and fully developed separation:

$h \geq 0.63$: incipient separation ($H_{12} \geq 2.7$)

$h \geq 0.75$: complete separation ($H_{12} \geq 4$).

Evolution of this parameter is indicated in table 1 for the case without vortex. It can be noticed that incipient separation occurs for x/c slightly lower than 0.4 and full separation for x/c = 0.45. The thickness parameter δ, characteristic of the boundary layer thickness is defined by the speed at which corresponds to 99% of the infinite speed. in our confined case this thickness is taken to the thickness at which the speed is equal to the maximum speed.

Table 1: Parameters of BL without vortex

x/c	δ (mm)	δ_1 (mm)	δ_2 (mm)	H_{12}	h	χ_{max} (%)
0,3	2,71	0,56	0,32	1,73	0,42	0
0,4	6,32	1,57	0,55	2,86	0,65	0,19
0,45	6,28	2,47	0,61	4,08	0,76	1,12

The backflow coefficient χ is defined by the percentage of time where speed is in opposite direction of that of the reference

velocity. The separated region is defined by Lögdberg [3] as the area where the backflow coefficient is larger than 0.5. This parameter is estimated using PIV data, since the interrogation areas must be large enough to contain approximately 5 particles. The first available χ values are determined 1mm from the wall and are significant when the BL thickness is large enough (i.e. in incipient or fully developed separated area).

Longitudinal Vortex

The vortex is generated by a 3D wing positioned 2 chord (2 c_{ell}) upstream of the zero incidence leading edge of the main hydrofoil. This generation method and foil characteristics have been chosen, first, because previous studies in the laboratory gave numerous data concerning the characteristics of such vortex (Pichon, [9]), and secondly, for convenience of implementation in the vein of the water tunnel. Indeed, the implementation of a mechanical system allowed us to control the characteristics of the vortex (intensity and position).

An experimental validation was performed, to verify that the wake of the 3D wing did not disturb the flow on the suction side of the profile. The incidence of the foil for the generation of the tip vortex was far enough from the separation to develop a thin wake. The validation showed that the signature of the 3D wing on the flow on the suction side of the 2D foil is hardly observable, and that therefore the assumption of isolated vortex is justified.

Mean axial and tangential velocity obtained by LDV was fitted using a theoretical model of vortex. The chosen model due to Batchelor [11], and developed to model the aircraft tip vortices, is a 3D extension of Lamb-Oseen model. This model is defined by the following equations:

$$U_r = 0$$

$$U_\theta = \frac{\Gamma}{2\pi r}\left(1-\exp\left(-\frac{r^2}{a^2}\right)\right)$$

$$U_z = U_0 - \frac{\Gamma}{2\pi l}\left(1-\exp\left(-\frac{r^2}{a^2}\right)\right)$$

This Batchelor model is illustrated in Figure 4. The experimental mean axial and tangential profiles are plotted and superimposed to the model in figure 5. As it is shown, Batchelor vortex is one of the most realistic models to represent a single vortex with axial flow.

Considering that the aim of this study was to focus on the BL modifications, only one configuration of vortex generation has been achieved. The incidence angle of the 3D NACA0020 was 8° for the upstream velocity of U_{inf} = 5.56 m/s.

The vortex trajectory was determined in the (x, y, z) coordinates where the origin of these axes was located at the extremity of the 3D foil. The vortex trajectory is plotted in Figure 6.

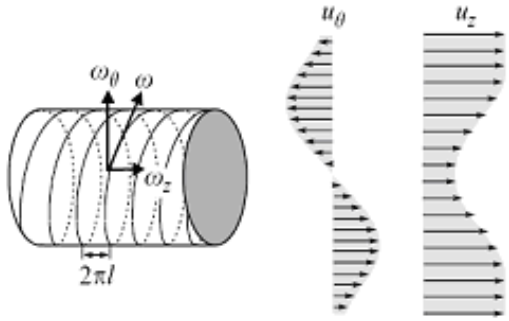

Figure 4: Scope of vorticity and the velocity induced by a model type Batchelor

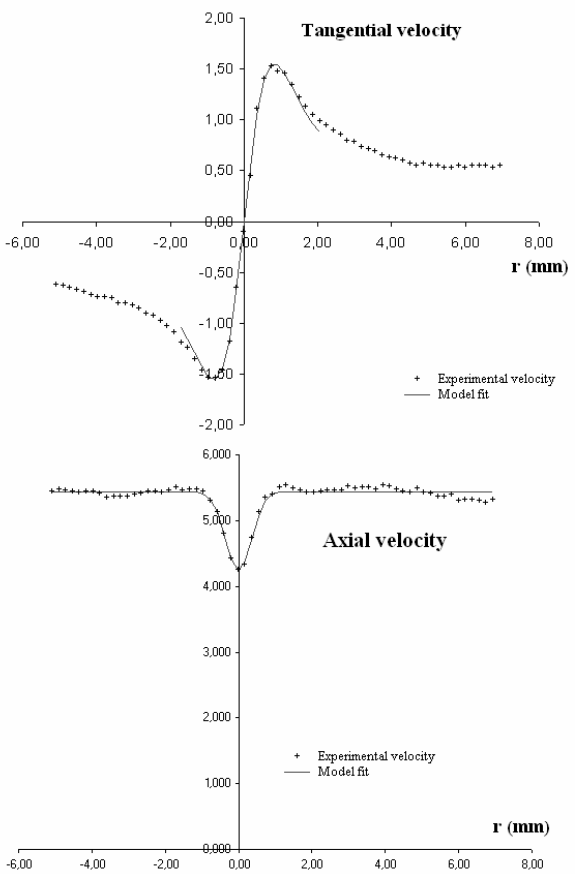

Figure 5: Example of tangential and axial velocity fit

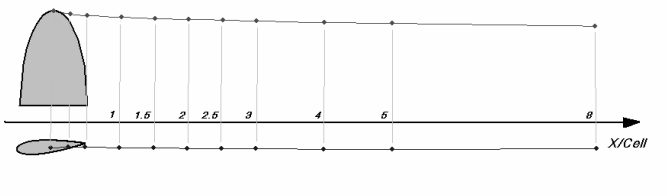

Figure 6: Trajectory of the vortex. Incidence 8° and U_{inf} = 5.56 m/s.

For selected points of the trajectory, circulation evolution (Γ) of the vortex has been done with normalized x-axis as it is shown in Figure 7. An increase of the vortex circulation with downstream direction associated with a growth of the vortex size and the decrease of the maximum tangential velocity and an increase of the helicity pitch was noticed. This behavior characterizes the vortex diffusion, ultimately leading to its disintegration.

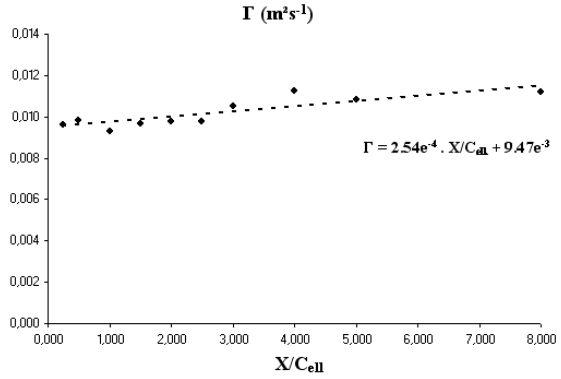

Figure 7: Evolution of Vortex Circulation depending on the distance to the free end

To estimate the axial flow compared to a characteristic velocity of the vortex rotation, the non dimensional number W_0 was used. This number characterized the vortex stability and is defined by:

$$W_0 = (U_0 - U_{\inf})\frac{2\pi a}{\Gamma}$$

and plotted in Figure 8. Note that $|W_0| < 0.6$ along the x-axis, this value is considered as stable by Fabre and Jacquin [12].

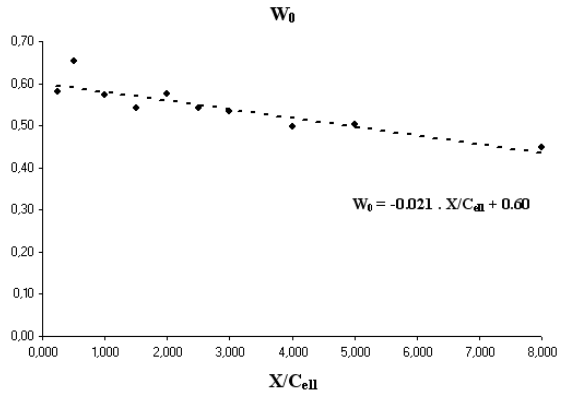

Figure 8: Stability of the vortex.

INTERACTION

Interaction parameters

Before analyse the interaction between vortex and BL, it was necessary to define three local parameters: d/δ, Γ/δU_e, a/δ. These parameters represent respectively the relative normal position of the vortex to BL, the non-dimensional circulation and the aspect ratio between the core vortex size and BL size. The evolutions of these three parameters with the position x/c are shown Figure 10 & 11. It can be noticed that d/δ is greater than 1, corresponding to the vortex outside the BL thickness.

Several studies (Angele et al. [6]) concerning the effect of vortices on BL pattern considered this parameter rather constant and always lower than 1 for all configurations. In our case, d/δ decreases along the boundary layer as the vortex is guided in the NACA0015 flow and perturbed by the pressure gradient induced by the 2D foil. It is smallest value (~1) is reached near the trailing edge of the 2D foil.

The presence of the NACA0015 foil induces a vortex deviation in the vertical (x-y) plane associated with the lifting flow generated by the 2D foil. This trajectory is shown in Figure 9. In the transversal (y-z) plane the vortex is slightly deviated due to the image effect. As the vortex is located quite far from the wall this effect remains of little importance.

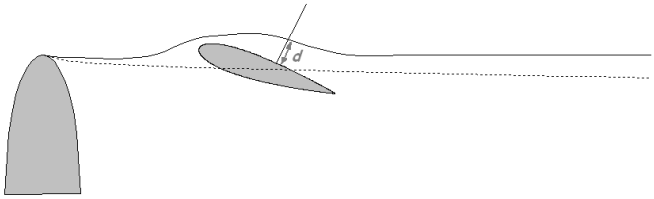

Figure 9: Trajectory of the tip vortex with downstream foil (solid line) and without (dotted line)

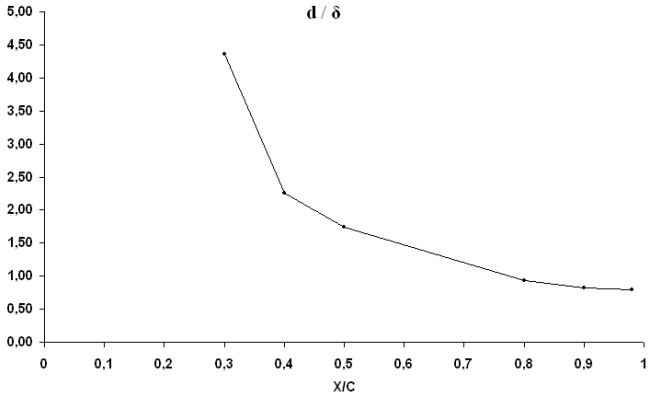

Figure 10: Non-dimensional distance between vortex and 2D foil

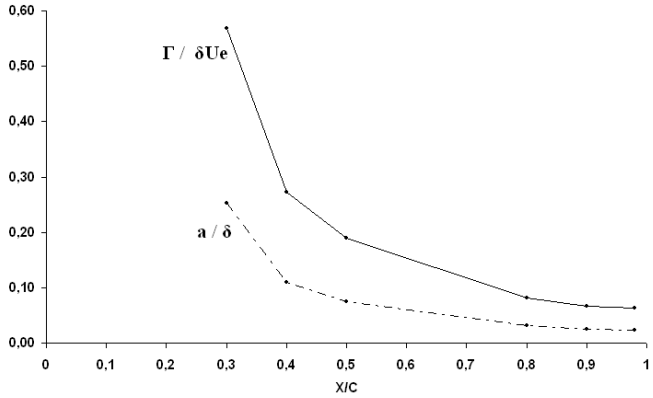

Figure 11: Non-dimensional circulation and aspect ratio

The relative normal position of the vortex and its relative circulation to BL, are shown Figure 10. The same trends as compared to the non-dimensional distance can be observed. These values can be compared with those obtained by Shabaka et al. [1] in the case of longitudinal vortices imbedded in turbulent boundary layers. They determined the ratio of Γ to Ue.δ downstream the VGs of about 0.054. In our case, this value is obtained through an asymptotic behaviour near the trailing edge. As it is expected, these values will provide a strong influence on the separation area.

Global efforts

Lift and drag measurements have been performed with and without vortex and are reported on Figure 12. Obviously the values of both lift and drag coefficients are not affected by the upstream vortex for incidences lower than 7°. Between 7° and 15° the lift coefficient remains unchanged but the drag coefficient increases rapidly.

For larger values of the angle of attack the hysteretic loop, characteristic of the static stall, disappears (Sarraf [8]) and the lift coefficient have a plateau like behaviour. The presence of the vortex induces a displacement of the detachment point, and their oscillations are inhibited.

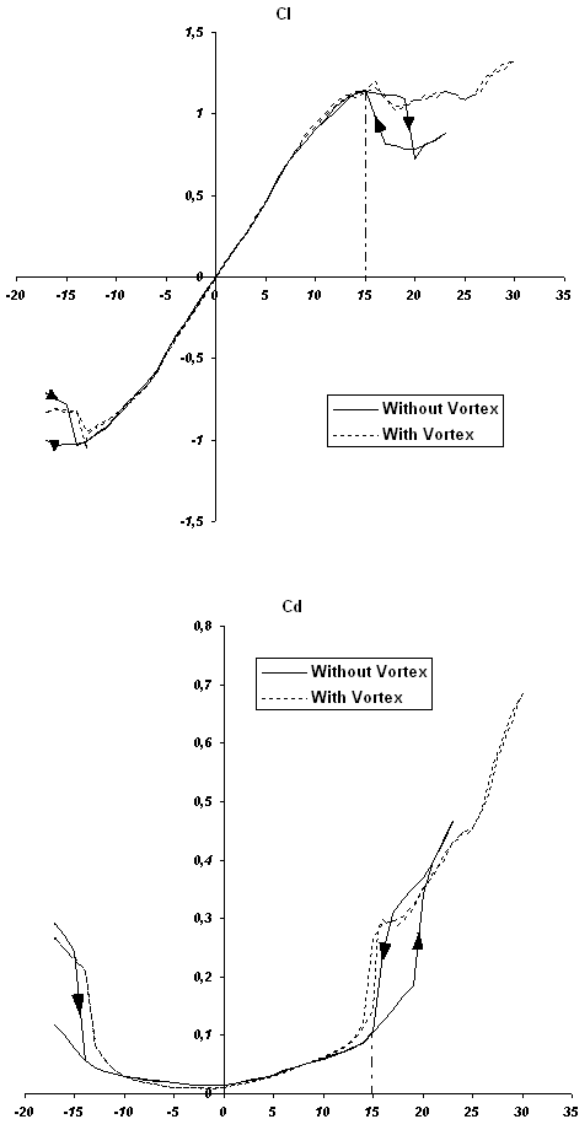

Figure 12: Global coefficient of lift Cl and Drag Cd

Interaction of the BL on the vortex

It can be seen in Figure 10 that the vortex gets nearer the BL at trailing edge. This trend is accentuated when incidence angle is increased.

The vortex circulation has been determined in the presence of the BL. Its evolution is shown Figure 13 versus normalized downstream direction x/cell and compared to the one obtained without BL. The grey area represents the NACA zone in the x-axis. Note that the vortex is disturbed upstream the 2D foil and the circulation is globally increased. This behavior is accentuated in the wake of the 2D foil probably due to APG influence.

Concerning the vortex stability, the W_0 value is increased in the NACA0015 area (corresponding to the Cp_{min} location on the 2D foil) and the vortex is strongly destabilized. Furthermore, W_0 is decreased upstream the 2D foil near the stagnation point.

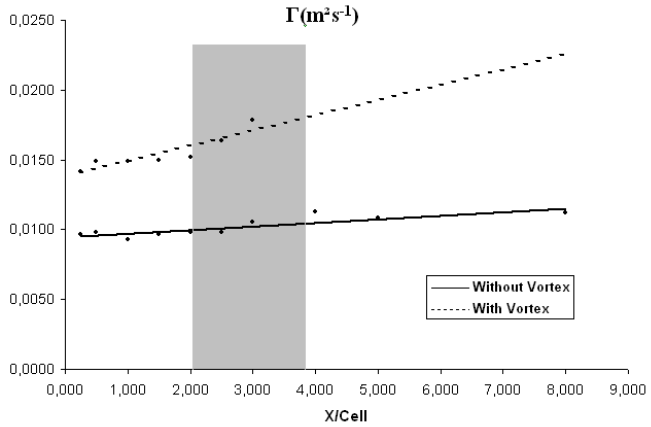

Figure 13: Evolution of Vortex Circulation with and without vortex.

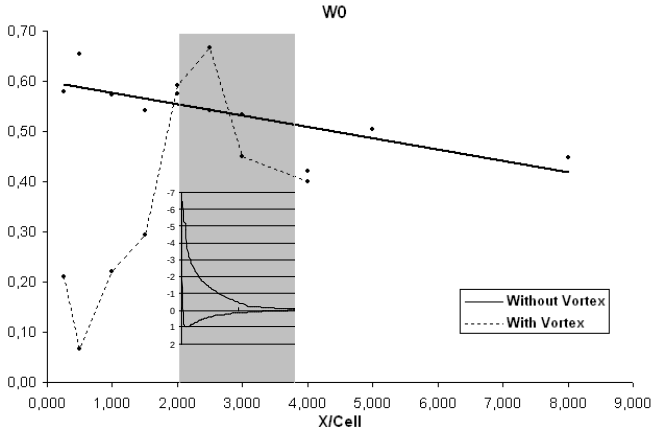

Figure 14: Evolution of stability parameter with and without vortex.

It can be noticed that the circulation (Figure 13) and the stability (Figure 14) parameter have been determined until x/Cell= 4 (corresponding to the location near the NACA0015 trailing edge).

Even the existence of the vortex is confirmed by the axial and tangential velocity, it is destructured and the Batchelor model is not justified. These results can be linked with the vortex breakdown associated to the APG due to the NACA0015 design and incidence angle. As described by Gursul and Yang [13] it is well known that there are two parameters which determine the breakdown location: the swirl angle and the external pressure gradient outside the vortex core. Hall [14] suggested that the vortex breakdown occurs as a result of APG along the vortex axis which leads to a stagnation point. Nevertheless, in our case the vortex coherence is sufficient to compensate the APG effects and continue to exist downstream the 2D foil. In fact, the breakdown is observed for higher incidences.

Interaction of the vortex on the BL

Shape factor is now analyzed to point out the effect of the vortex on the BL. The h values corresponding to classical incipient detachment and complete separation are also reported. Figure 15 shows the h evolution versus x/c with and without vortex at different transverse position (inflow and outflow zones).

It can be noted that, in the inflow region the boundary layer is attached until x/c=0.7 and the shape value is close to the one obtained in turbulent boundary layer case.

In the outflow region the complete separation is reached for x/c= 0.65 instead of x/c=0.45 without vortex. As it is expected in the inflow region the vortex considerably delays the separation near the trailing edge by the transfer of momentum in the boundary layer with a delay to reach separation (Velte et al. [6]).

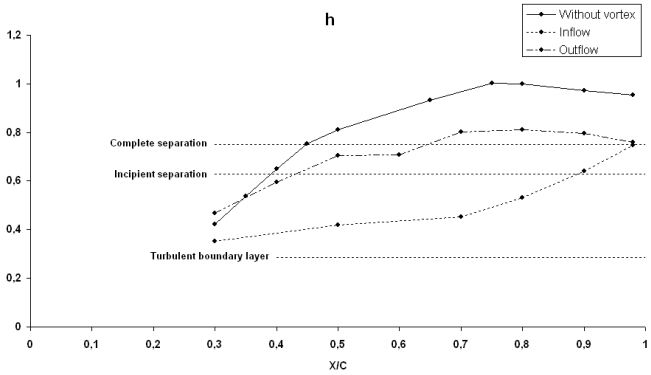

Figure15: h coefficient for the case without and with vortex.

The following figures (Figure 16(a)(b)(c)) show the evolution of the backflow coefficient χ superimposed with normalized velocity U/U_{inf}, the boundary layer thickness (δ) and the vortex position (d) with and without vortex. It can be seen from this figure that the trends described by Logdberg are not reproduced in the case of the present results. Essentially, the criteria of separation (χ=0.5) is not in agreement with our results even if the principal trends concerning correlation between the mean velocity defect and the maximum of backflow coefficient remain the same. Obviously the vortex induces a decrease of the maximum backflow value observed even in the outflow region and this maximum is observed further downstream in this case showing the effectiveness of the vortex to decrease the extent of the separated area.

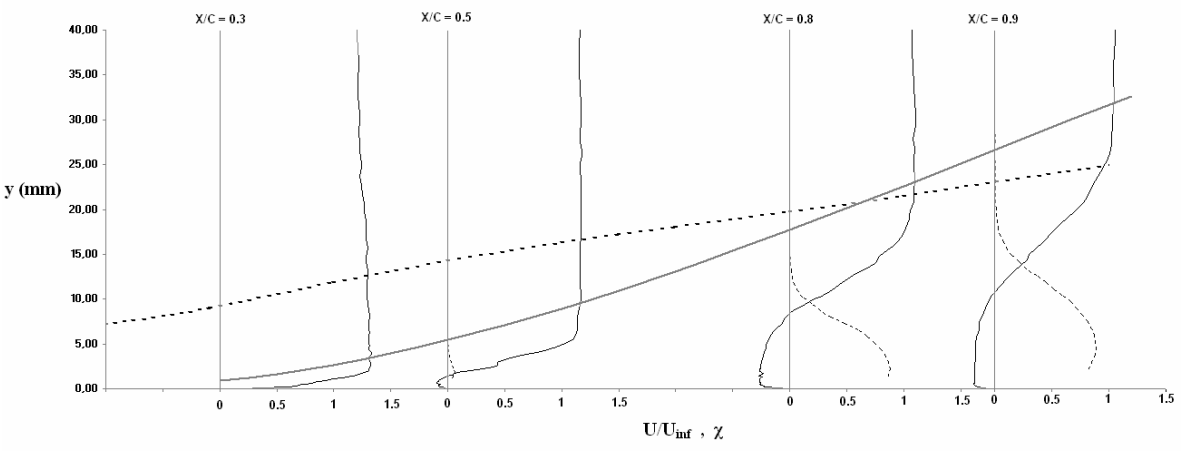

(a) Without Vortex

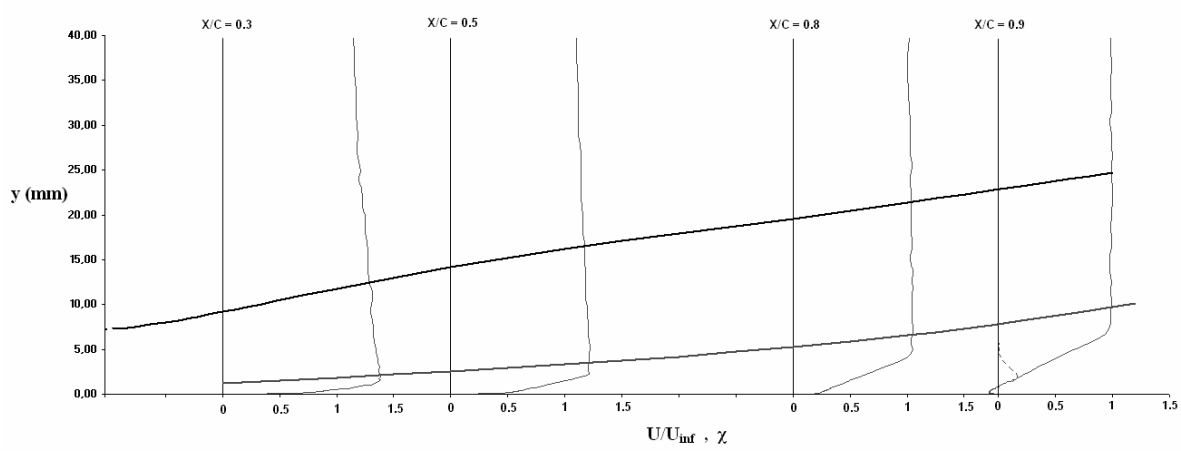

(b) With vortex Inflow region

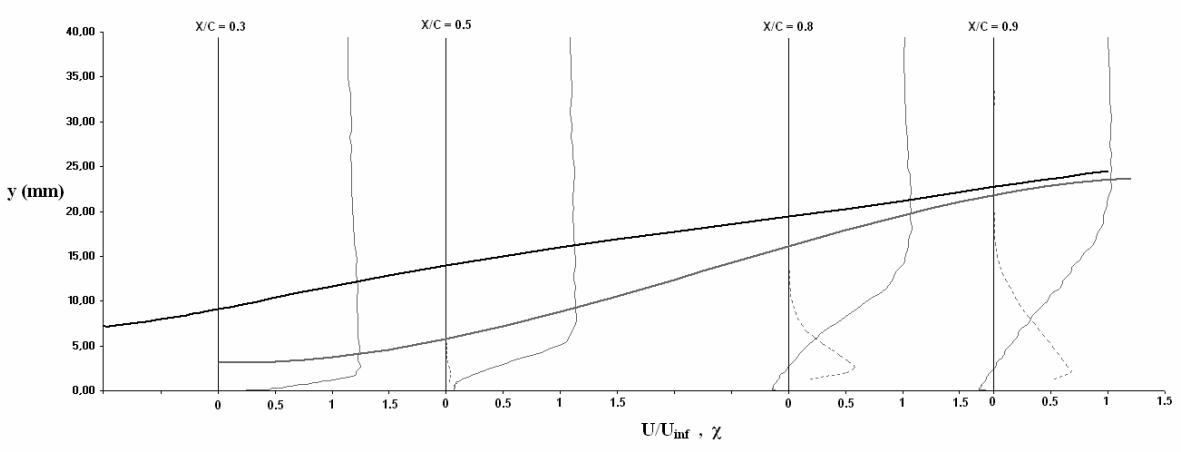

(b) With vortex Outflow region

Figure16: Boundary layer and separation zone for three cases, without vortex (a), with vortex Inflow (b) and Outflow (c).
The figure is not to scale in the X direction for more visibility. The grey full lines show U/U_{inf}, the grey dashed-dotted lines show the backflow coefficient χ. The grey full thick lines show the δ parameter of boundary layer. The black full lines represent the trajectory of the vortex, and the black dashed-dotted lines show the virtual position of the vortex in the case without vortex.

SUMMARY AND CONCLUSION

The results of the actual work provide us a survey of a boundary layer that develops on a 2D NACA0015 foil with and without longitudinal vortex passing in the vicinity of the boundary layer.

As a conclusion the presence of the vortex has a major effect both on the boundary layer and on the global parameters. We have shown that the hysteretic behavior of the global parameters (lift and drag) is inhibited by the presence of the vortex. The lift stress is suppressed and replaced by a plateau where the lift value is equivalent to the maximum lift value in the case without vortex.

This effect is related to the modification of the flow on the suction side of the foil where, both in the inflow or outflow region where the extension of the separated area, both is decreased. This effect is greater in the inflow region even if it remains observable in the outflow region. These effects are induced by the momentum exchanges induced by the vortex between the external and internal regions of the boundary layer with an input of external fluid in the boundary layer in the inflow region and an extraction of slow fluid from the boundary layer in the outflow region.

These effects can be used to control the flow on the 2D hydrofoil.

ACKNOWLEDGMENTS

We would like to thank the company *Dantec Dynamics* for their great help and more particularly J-J. Lasserre, O. Pust, A. Poidatz, and P. Galletier, for their support through the sharing of their know-how and the provision of hardware necessarily for the realization of measurements of PIV 2D3C.

REFERENCES

[1] I. M. M. A. Shabaka, R. D. Mehta & P. Bradshaw. *Longitudinal vortices imbedded in turbulent boundary layers. Part 1. Single vortex* J. Fluid Mech. 155, 37–57.

[2] R. D. Mehta & P. Bradshaw. *Longitudinal vortices imbedded in turbulent boundary layers. Part 2. Vortex pair with common flow upwards* J. Fluid Mech. 188, 529-546.

[3] O. Löbdberg. *Turbulent boundary layer separation and control*. Technical Reports from Royal Institute of Technology KTH, Mechanics. 2008.

[4] K. P. Angele & B. Muhammad-Klingmann. *The effect of streamwise vortices on the turbulence structure of a separating boundary layer*. Europ. J. Mech. B/Fluids, vol. 24. pp. 539-554. 2005.

[5] K. P. Angele, F. Grewe, *Instantaneous behaviour of streamwise vortices for turbulent boundary layer separation control*, Journal of Fluid Engineering, Vol. 129(2), 2007.

[6] C.M. Velte, M.O.L. Hansen and D. Cavar. *Flow analysis of vortex generators on wing sections by stereoscopic particle image velocimetry measurements*. Environ. Res. Lett. 3, 2008.

[7] C. M. Velte. *Characterization of Vortex Generator Induced Flow*. PhD thesis, Fluid Mechanics Department of Mechanical Engineering Technical University of Denmark. 2009.

[8] C. Sarraf, H. Djeridi, S. Prothin, J-Y. Billard, *Thickness effect of NACA foils on hydrodynamic global parameters, boundary layer states and stall establishment*, Journal of Fluids and Structures, in press YJFLS-1175.

[9] T. Pichon, *Contribution à l'étude de la Cavitation de Tourbillon Marginal*. PhD thesis, Ecole Centrale de Nantes, 1995.

[10] S.J. Kline, J.G. Bardina, R.C. Strawn, *Correlation of the Detachment of Two-dimensional Turbulent Boundary Layers*, AIAA J., vol. 21, 1983, p. 68.

[11] G. K. Batchelor. *Axial flow in trailing line vortices*. J. Fluid Mech. 20, 645–658. 1964.

[12] D. Fabre & L. Jacquin. *Viscous instabilities in trailing vortices at large swirl numbers*. J. Fluid Mech. 500, 239–262. 2004.

[13] I. Gursul & H. Yang. *Vortex breakdown over a pitching delta*. Journal of Fluids and Structures. Vol. 9, pp. 571-583. 1995.

[14] M. G. Hall. *Vortex breakdown*. Annual review of fluid Mechanics 4, pp. 195-218. 1972.